EC Journals.ASM.org

N-Terminal Presequence-Independent Import of Phosphofructokinase into Hydrogenosomes of *Trichomonas vaginalis*

Petr Rada,[a] Abhijith Radhakrishna Makki,[a] Verena Zimorski,[b] Sriram Garg,[b] Vladimír Hampl,[a] Ivan Hrdý,[a] Sven B. Gould,[b] Jan Tachezy[a]

Department of Parasitology, Charles University in Prague, Faculty of Science, Prague, Czech Republic[a]; Institute for Molecular Evolution, Heinrich-Heine-University Düsseldorf, Düsseldorf, Germany[b]

Mitochondrial evolution entailed the origin of protein import machinery that allows nuclear-encoded proteins to be targeted to the organelle, as well as the origin of cleavable N-terminal targeting sequences (NTS) that allow efficient sorting and import of matrix proteins. In hydrogenosomes and mitosomes, reduced forms of mitochondria with reduced proteomes, NTS-independent targeting of matrix proteins is known. Here, we studied the cellular localization of two glycolytic enzymes in the anaerobic pathogen *Trichomonas vaginalis*: PP_i-dependent phosphofructokinase (*Tv*PP_i-PFK), which is the main glycolytic PFK activity of the protist, and ATP-dependent PFK (*Tv*ATP-PFK), the function of which is less clear. *Tv*PP_i-PFK was detected predominantly in the cytosol, as expected, while all four *Tv*ATP-PFK paralogues were imported into *T. vaginalis* hydrogenosomes, although none of them possesses an NTS. The heterologous expression of *Tv*ATP-PFK in *Saccharomyces cerevisiae* revealed an intrinsic capability of the protein to be recognized and imported into yeast mitochondria, whereas yeast ATP-PFK resides in the cytosol. *Tv*ATP-PFK consists of only a catalytic domain, similarly to "short" bacterial enzymes, while *Sc*ATP-PFK includes an N-terminal extension, a catalytic domain, and a C-terminal regulatory domain. Expression of the catalytic domain of *Sc*ATP-PFK and short *Escherichia coli* ATP-PFK in *T. vaginalis* resulted in their partial delivery to hydrogenosomes. These results indicate that *Tv*ATP-PFK and the homologous ATP-PFKs possess internal structural targeting information that is recognized by the hydrogenosomal import machinery. From an evolutionary perspective, the predisposition of ancient ATP-PFK to be recognized and imported into hydrogenosomes might be a relict from the early phases of organelle evolution.

The transition of the mitochondrion into an ATP-producing organelle was the crucial event at the eukaryote origin (1). ATP synthesis in eukaryotes is typically compartmentalized, with glycolysis in the cytosol and pyruvate oxidation in the mitochondria, which is linked to highly efficient oxidative phosphorylation (1, 2). In protists, however, there are notable exceptions to the usual scheme regarding both glycolysis and pyruvate oxidation. In *Trichomonas vaginalis* and other eukaryotes that possess an anaerobic form of mitochonria called hydrogenosomes, pyruvate is oxidized within the organelle via less efficient anaerobic fermentation (3). *Giardia intestinalis*, *Entamoeba histolytica*, and other eukaryotes possess a reduced form of mitochondria called mitosomes that do not produce ATP at all (4). In these organisms, pyruvate oxidation takes place exclusively in the cytosol (1). In kinetoplastids, glycolysis is compartmentalized in specialized microbodies called glycosomes (5). In some green algae, the first half of the glycolytic pathway is localized in the chloroplast (6, 7), while in the diatom *Phaeodactylum tricornutum* and other stramenopiles, several glycolytic enzymes are targeted to multiple compartments, such as the cytosol, plastids, and mitochondria (8, 9).

A particularly vexing case of compartmentalization involves *T. vaginalis* phosphofructokinase (PFK). In *Trichomonas*, glycolysis proceeds via a pyrophosphate (PP_i)-dependent phosphofructokinase (PP_i-PFK) (10), an enzyme that is generally rare in eukaryotes, albeit typical in plants (11). Therefore, it was surprising that genes for ATP-dependent phosphofructokinase (ATP-PFK) turned up in the *Trichomonas* genome (12). Furthermore, peptides of the expressed protein were found in the hydrogenosomal proteome (13–15), although the exact topology of hydrogenosome-associated *T. vaginalis* ATP-PFK (*Tv*ATP-PFK) remains unclear (13, 15). PP_i-PFK and ATP-PFK share an evolutionary origin (16, 17). In bacteria, ATP-PFK is a homo-oligomeric enzyme that is formed by ~35-kDa subunits (18). In opisthokonts, ATP-PFK underwent gene duplication and fusion events, resulting in an ~90-kDa protein with an N-terminal catalytic domain and a C-terminal regulatory domain (19). The PP_i-PFK protein forms homo- or, in plants, heterotetramers of ~40- to 60-kDa subunits, and in Apicomplexa, the two subunits are fused to a protein of ~140 kDa (20). The advantage of using PP_i-PFK rather than ATP-PFK in glycolysis lies in the increased yield of ATP due to the replacement of ATP with PP_i as a phosphate donor in the phosphorylation of fructose-6-phosphate (3). This is particularly important for *T. vaginalis* and other anaerobes with energy metabolism based mainly on glycolysis (10).

In most eukaryotes, the N-terminal targeting sequences (NTS) are required for the delivery of nuclear-encoded proteins into the mitochondrial matrix, whereas the NTS-independent pathway is mainly involved in the routing of proteins into the outer and inner mitochondrial membranes and the intermembrane space. NTS are typically 15 to 55 residues in length and form a positively

Received 4 July 2015 **Accepted** 8 October 2015

Accepted manuscript posted online 16 October 2015

Citation Rada P, Makki AR, Zimorski V, Garg S, Hampl V, Hrdý I, Gould SB, Tachezy J. 2015. N-terminal presequence-independent import of phosphofructokinase into hydrogenosomes of *Trichomonas vaginalis*. Eukaryot Cell 14:1264–1275. doi:10.1128/EC.00104-15.

Address correspondence to Jan Tachezy, tachezy@natur.cuni.cz.

Supplemental material for this article may be found at http://dx.doi.org/10.1128/EC.00104-15.

charged amphipathic α-helix (21). Upon preprotein delivery into the matrix by the outer (TOM) and inner (TIM) membrane translocases, the NTS is removed by a heterodimeric zinc-dependent mitochondrial processing peptidase (MPP) (22). Proteins routed by the NTS-independent pathway possess either a single or multiple internal targeting signals (ITS) (23). In *Saccharomyces cerevisiae* and human mitochondria, the components and mechanisms of protein import via the NTS-dependent pathway are well characterized (23), whereas less is known about protein import in hydrogenosomes. The NTS-dependent mechanism is present in hydrogenosomes and mitosomes (4, 24, 25), but a few studies have also reported NTS-independent import into the hydrogenosomes of *T. vaginalis* (26, 27, 58).

Interestingly, there are four ~35-kDa *Tv*ATP-PFK proteins encoded in the *T. vaginalis* genome, none of which possesses an NTS. The multiple copies preclude the generation of *Tv*ATP-PFK knockouts with current *Trichomonas* tools to study their functions, which remain mysterious. To clarify the localization and exact organellar topology of *Tv*ATP-PFK, we investigated the targeting of products encoded by *Tv*ATP-PFK genes when expressed in transformed *T. vaginalis* cells using immunofluorescence microscopy and cell fractionation, characterized the ATP dependence of *Tv*ATP-PFK import into isolated hydrogenosomes, and tested whether *Tv*ATP-PFK could be recognized as a substrate for NTS-independent import into yeast mitochondria. Conversely, we assessed whether the homologous catalytic domain of yeast ATP-PFK, as well as ~35-kDa *Escherichia coli* ATP-PFK (*Ec*ATP-PFK), showed a tendency to be imported into hydrogenosomes when expressed in *T. vaginalis*.

MATERIALS AND METHODS

T. vaginalis strain T1 (provided by J.-H. Tai, Institute of Biomedical Sciences, Taipei, Taiwan) was grown in Diamond's tryptone-yeast extract-maltose (TYM) medium supplemented with 10% (vol/vol) heat-inactivated horse serum. *S. cerevisiae* strain INVSc1 (Invitrogen) was grown in yeast extract-peptone-dextrose (YPD) medium or minimal medium devoid of uracil when transfected.

Phylogenetic analyses. The sequences of ATP-PFK and PP_i-PFK in a wide diversity of prokaryotes and eukaryotes were downloaded from the protein and EST database of GenBank release 200.0 and aligned with the *T. vaginalis* sequences with MAFFT (28; http://mafft.cbrc.jp/alignment/server/) using an L-INS-i strategy. The alignment was manually edited using BioEdit 7.0.9.0 (29), and 340 well-aligned positions were used for the subsequent analyses. The phylogenetic tree was constructed by the maximum-likelihood method in RAxML version 7.2.8 (30) using the PROTGAMMALGF model on the RAxML black box server (31). The statistical support was assessed by bootstrapping with 100 repetitions in RAxML. Bayesian posterior probabilities were calculated in Phylobayes (32) on the CIPRES Science Gateway v. 3.3 (http://www.phylo.org/index.php/). Two chains of Markov chain Monte Carlo were run under the CAT GTR model with a sampling frequency of 1,800. The run was terminated when the discrepancy observed across all bipartitions (maxdiff) dropped below 0.3 and effective sizes were larger than 50. The first 500 trees were discarded as burn in, and a consensus tree with posterior probabilities was calculated from the sample of 14,080 trees.

Gene cloning and transformation. Selected genes (*Tv*ATP-PFK1, TVAG_293770; *Tv*PP_i-PFK1, TVAG_430830; *T. vaginalis* ferredoxin 1 [Fdx1], TVAG_003900; *S. cerevisiae*ATP-PFK [*Sc*ATP-PFK], DAA08331; and *E. coli Ec*ATP-PFK, EFJ85506.1) were amplified by PCR from *T. vaginalis* and *S. cerevisiae* genomic DNA and cloned into the plasmids (i) pTagVag2, enabling the expression of the inserted genes with a C-terminal dihemagglutinin (di-HA) tag in trichomonads (33), and (ii) a self-modified version of plasmid pYES2/CT that allows the expression of the inserted genes with C-terminal green fluorescent protein (GFP) in yeasts. Transformed trichomonads and *S. cerevisiae* cells were selected as previously described (33, 34). The primers that were used for amplification and cloning of the selected genes into the pTagVag2 and pYES2/CT plasmids are shown in the supplemental material.

The pTagVag2 plasmid allows expression of the inserted genes under the control of the *T. vaginalis* hydrogenosomal α-subunit succinyl-coenzyme A (CoA) synthetase (SCSα) gene promoter (33). Alternatively, we used native promoters of selected genes instead of the SCSα promoter. The selected genes were amplified by PCR with 300 bp of upstream noncoding sequences and inserted into the pTagVag2 plasmid with a deleted SCSα promoter (pTagVagN). The primers used to amplify and clone the selected genes with their native promoters are shown in the supplemental material.

Immunofluorescence microscopy. Episomally expressed recombinant proteins were detected in trichomonads using a monoclonal mouse anti-HA antibody (35). In double-labeling experiments, hydrogenosomal malic enzyme was detected using a rabbit polyclonal antibody (36). A secondary Alexa Fluor 488 (green) donkey anti-mouse antibody and Alexa Fluor 594 (red) donkey anti-rabbit antibody were used for visualization of target proteins. The cells were examined using an Olympus Cell-R IX81 microscope system. The acquired images were processed using ImageJ software (version 1.4d) (http://rsbweb.nih.gov/ij/). In *S. cerevisiae* cells, episomally expressed recombinant proteins with GFP were detected and examined as described above. In double-labeling experiment, mitochondria were detected with MitoTracker dye (Invitrogen).

Enzyme assays. ATP-PFK activity was determined in the glycolytic direction using a continuous spectrophotometric assay according to the method of Chi et al. (37) with some modifications. The assay mixture for ATP-PFK consisted of 2 ml of 100 mM HEPES, 50 mM KCl, 3 mM $MgCl_2$, 1 mM EDTA, pH 7.0, buffer; 1 mM ATP; 20 mM fructose-6-phosphate; 0.15 to 0.20 mM NADH; 2 to 3 U each of aldolase, triosephosphate isomerase, and glycerol-3-phosphate dehydrogenase (Sigma-Aldrich); and 0.05% (vol/vol) Triton X-100 (ATP-PFK assay buffer). The assay was performed in 1-cm anaerobic cuvettes. The reaction was started by alternatively adding ATP, fructose-6-phosphate, auxiliary enzymes, or protein sample to the assay mixture, and the reaction was monitored as a decrease in the absorbance of NADH at 340 nm using a Shimadzu UV-2600 spectrophotometer. PP_i-PFK activity was determined as previously described (38). The protein concentrations in the subcellular fractions of *T. vaginalis* were determined by the Lowry protein assay.

Preparation of cellular fractions. Highly purified hydrogenosomes were obtained from *T. vaginalis* total cell lysates by differential and Percoll gradient centrifugation as described previously (35). The cytosolic fraction was isolated according to the method of Sutak et al. (35) and subsequently centrifuged at 190,000 × *g* (the high-speed cytosolic fraction). Mitochondria of *S. cerevisiae* were isolated from the yeast according to the method of Gregg et al. (39).

Protease protection assay. Aliquots of intact hydrogenosomes (3 mg) were resuspended in 1 ml of 1× ST buffer (250 mM sucrose, 10 mM Tris, pH 7.8, 0.5 mM KCl) supplemented with protease inhibitor cocktail tablets (Roche Complete, EDTA free). Trypsin (Sigma) was added to a final concentration of 200 μg/ml, and the samples were incubated at 37°C for 30 min. After incubation, the trypsin activity was stopped by the addition of soybean inhibitors (5 mg/ml), and the samples were analyzed by immunoblotting with a monoclonal mouse anti-HA antibody.

Aliquots of intact mitochondria (1 mg) were resuspended in 1 ml of SEM buffer (1 mM MOPS [morpholinepropanesulfonic acid]-KOH, pH 7.2, 250 mM sucrose, 1 mM EDTA). Proteinase K (Sigma) was added to a final concentration of 50 μg/ml, and the samples were incubated at 37°C for 30 min. After incubation, the proteinase K activity was stopped by the addition of 250 μl of trichloroacetic acid. The samples were analyzed by immunoblotting with a monoclonal anti-GFP antibody (Pierce).

Preparation of radiolabeled precursor proteins. The *Tv*ATP-PFK1 gene was cloned into the modified psp64 poly(A) plasmid, which enables

in vitro mRNA synthesis from the inserted genes (Promega). The primers designed for PCR and cloning into the psp64 plasmid are described in the supplemental material. *In vitro* transcription was performed using the mMachine kit (Ambion). [^{35}S]methionine-radiolabeled precursor protein was synthesized *in vitro* using the Flexi Rabbit Reticulocyte Lysate System (Promega).

In vitro import. Each *in vitro* import assay was performed in a reaction mixture that included 100 μl of import buffer (10 mM HEPES, pH 7.4, 250 mM sucrose, 2 mM KP_i, pH 7.4, 25 mM KCl, 10 mM $MgCl_2$, 0.5 mM EDTA, pH 8.0, 1 mM dithiothreitol [DTT], 10 mM ATP), 50 μl of cytosolic extract, 5 μl of radiolabeled precursor protein, and 5 mg of isolated hydrogenosomes. Apyrase (20 U/ml) was used for the import assay, which was conducted in the absence of ATP. The organelles were preincubated for 10 min at 25°C in import buffer with cytosolic extract, after which radiolabeled precursor protein was added to the assay mixture, and the mixture was incubated for 1, 10, and 60 min at 25°C. At each time point, the *in vitro* import was stopped by the addition of 100 μg/ml of proteinase K and placed on ice for 20 min. After incubation, the activity of proteinase K was inhibited by adding 2 mM phenylmethylsulfonyl fluoride (PMSF) (Sigma). The hydrogenosomes were then washed in import buffer and solubilized in SDS loading buffer. To test the activity of proteinase K, after a 60-min incubation of the protein import reaction mixture, the hydrogenosomes were dissolved with 0.5% (vol/vol) Triton X-100, followed by the addition of 100 μg/ml of proteinase K. Proteins in the supernatant were precipitated with methanol-chloroform and solubilized in SDS loading buffer. All of the samples were subjected to SDS-PAGE in a 13.5% separating gel. The gels were vacuum dried and exposed to X-ray films.

RESULTS

Phylogenetic analysis reveals the presence of PP_i-PFK and the short type of ATP-PFK in *T. vaginalis* and other parabasalids. The *T. vaginalis* genome possesses 11 genes encoding phosphofructokinases, four of which encode "short" (~35-kDa)-type ATP-dependent PFKs (*Tv*ATP-PFK1 to -4 [TVAG_293770, TVAG_496160, TVAG_462920, and TVAG_391760]) and seven of which encode PP_i-dependent PFKs (*Tv*PP_i-PFK1 to -7 [TVAG_430830, TVAG_077440, TVAG_281070, TVAG_364620, TVAG_079260, TVAG_263690, and TVAG_335880]). A phylogenetic analysis of ATP-PFKs and PP_i-PFKs revealed that *Trichomonas Tv*ATP-PFK1 to -4 fall into the single robust clade T2, together with PFKs from other parabasalids (Fig. 1). The closest eukaryotic relatives of this clade are tandem-fusion PFKs from opisthokonts and amoebozoans (clade E), as well as enzymes from prokaryotes (clades B1 and B2). The *Trichomonas* homologues *Tv*PP_i-PFK1 to -7 also form a clade with parabasalian sequences (Fig. 1). This parabasalian clade (clade T1) branches with enzymes from jakobids, heteroloboseans, and prokaryotes. The presence of both versions of the enzyme in other parabasalids suggests that both PP_i-PFK and ATP-PFK were present in the parabasalid ancestor. The branching of the *T. vaginalis* sequences in several unrelated positions in both clades T1 and T2 indicates that the genes have undergone gene duplications and possibly gene losses within parabasalids. The specificity of both types of PFKs for either ATP or PP_i has been ascribed to the amino acid residues at positions 104 and 124 (according to the numbering of the *E. coli Ec*ATP-PFK [40]). The G_{104} ($GGDG_{104}$ motif) and G/K_{124} residues are important for ATP binding, whereas PP_i binding requires residues D_{104} ($GGDD_{104}$ motif) and K_{124} (10, 17). *Tv*ATP-PFK1, -3, and -4 contain glycine at position 104, and *Tv*ATP-PFK1 and -3 contain glycine at position 124, whereas *Tv*ATP-PFK4 contains an alanine residue at the latter position (Fig. 2; see Fig. S2 in the supplemental material). The interchange of the glycine residue with alanine should not affect the interaction with the ATP molecule. The alanine residue possesses a small side chain, and it is unlikely that the residue creates steric hindrance to prevent binding of the ATP molecule. However, *Tv*ATP-PFK2 contains threonine and serine residues at positions 104 and 124, respectively. Therefore, the ability of *Tv*ATP-PFK2 to bind ATP is uncertain. The expected amino acid residues (D_{104} and K_{124}) are present in *Tv*PP_i-PFK1 and -3 to -6, whereas *Tv*PP_i-PFK2 and -7 contain glutamic acid and alanine residues at position 104, respectively (Fig. 2; see Fig. S2 in the supplemental material). Interestingly, scanning of the alignment of a broad range of sequences that were used for the phylogenetic analysis (Fig. 1) revealed the presence of paralogous genes with canonical G/D_{104} and G/K_{124} amino acid residues and with different residues at these positions in other parabasalids of clade T2 and in members of the Embryophyta, clade P. For example, serine residues at position 124 are also present in the putative ATP-PFKs of *Tritrichomonas foetus* and *Histomonas meleagridis* (see Fig. S2 in the supplemental material). Moreover, the *H. meleagridis* protein contains asparagine at position 104. These sequences, together with *Tv*ATP-PFK2 and -4, form the upper branch of clade T2 (Fig. 1). The unusual paralogues of Embryophyta PP_i-PFK-like sequences contain threonine/isoleucine and valine at positions 104 and 124, respectively (see Fig. S2 in the supplemental material), and they are grouped in the upper Embryophyta branch of clade P (Fig. 1). The functions of plant PP_i-PFK-like proteins are unknown (41).

Cellular localization of *Tv*ATP-PFK paralogues. The analysis of *Tv*ATP-PFK1 to -4 revealed an absence of sequence motifs thought to target precursors to hydrogenosomes. The *Tv*ATP-PFK sequences are colinear with their bacterial orthologues, lacking a predictable NTS and the cleavage site for the processing peptidase (Fig. 2). We found no internal motifs for subcellular targeting, and PSORT II predicted *Tv*ATP-PFKs to localize to the cytosol.

The subcellular localization of *Tv*ATP-PFK1 to -4 was investigated by the transient expression of C-terminally HA-tagged proteins in *T. vaginalis*. Immunofluorescence microscopy revealed that recombinant *Tv*ATP-PFK1, -2, and -4 colocalized with malic enzyme, the hydrogenosomal marker protein (Fig. 3; see Fig. S1 in the supplemental material), which suggested that these three proteins were transported into the hydrogenosomal matrix (we were unable to detect any expression of *Tv*ATP-PFK3 after several independent rounds of transfection). The topology of *Tv*ATP-PFK1 was further tested by protease protection assays. The treatment of isolated organelles with trypsin had no effect on the *Tv*ATP-PFK1 signal in the Western blot analysis, and the signal disappeared only in response to treatment with detergent (Fig. 3B). This finding indicates that *Tv*ATP-PFK is imported into *T. vaginalis* hydrogenosomes and is not associated with the organelle surface.

Although the bioinformatics analysis did not predict the presence of a cleavable NTS, we cannot exclude the possibility that a noncleavable "cryptic" NTS signal might direct *Tv*ATP-PFK1 to hydrogenosomes. Therefore, we expressed a truncated version of *Tv*ATP-PFK1 that lacked the first 16 amino acid residues (aa) (double the size of the known NTS in Fdx1). The truncated *Tv*ATP-PFK1 was delivered to the hydrogenosomes as its complete form (Fig. 3). This result confirmed that import of *Tv*ATP-PFK1 into hydrogenosomes is NTS independent. The expression of *Tv*PP_i-PFK revealed a cytosolic localization of the enzyme, as expected (Fig. 3).

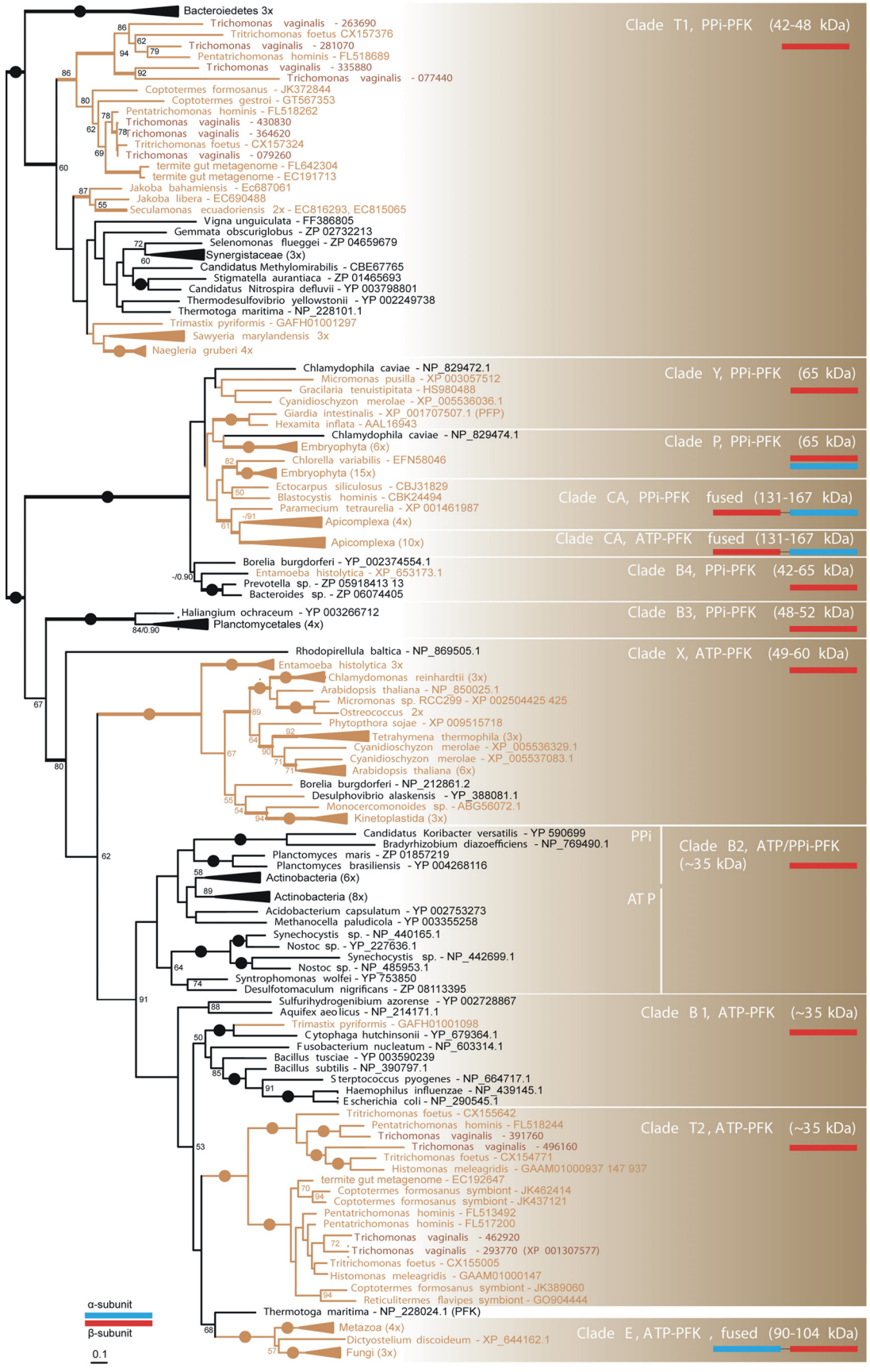

FIG 1 Phylogeny of ATP- and PP_i-dependent PFKs. Shown s a maximum-likelihood (ML) tree of PFK (191 taxa and 340 sites). The numbers at the nodes indicate bootstrap values (BV)/posterior probabilities (PP). Only BV and PP greater than 50% and 0.9, respectively, are shown. Branches with BV of >95% are marked by black circles, and branches with PP of >0.95 are marked by thick lines. Substrate specificity, molecular mass, and subunit composition for clades are indicated. The names of eukaryotes are in brown, and those of prokaryotes are in black.

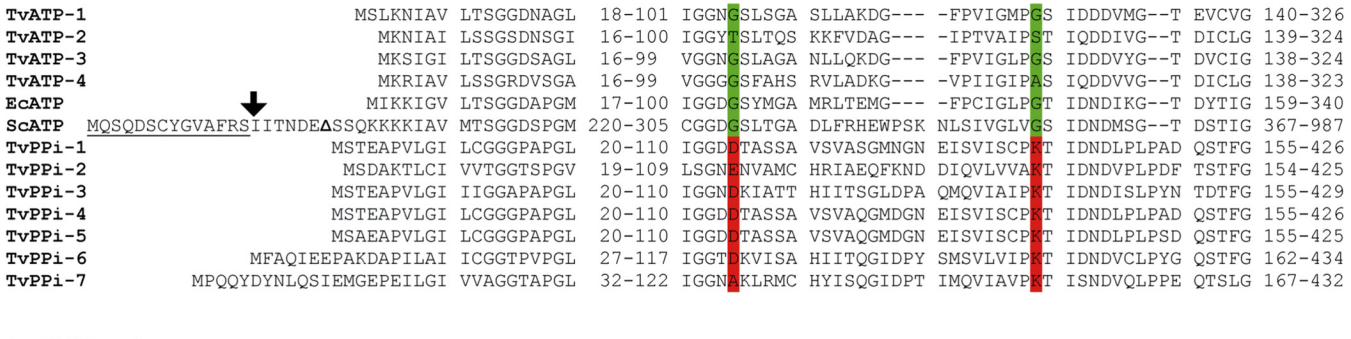

FIG 2 Multiple-protein-sequence alignment of the N-terminal portions and ATP/PP_i binding domains of *T. vaginalis* ATP- and PP_i-dependent PFKs. *T. vaginalis* TrichDB accession numbers: *Tv*ATP-PFK1 to -4, TVAG_293770, TVAG_496160, TVAG_462920, and TVAG_391760; *Tv*PP_i-PFK1 to -7, TVAG_430830, TVAG_077440, TVAG_281070, TVAG_364620, TVAG_079260, TVAG_263690, and TVAG_335880. NCBI accession numbers: *E. coli*, NP_418351; *S. cerevisiae*, DAA08331. A PSORT II-predicted NTS in *Sc*ATP-PFK is underlined; the arrow indicates the predicted cleavage site. The amino acid residues that are required for the interaction with ATP are shaded in green, and the residues that are crucial for the interaction with a PP_i molecule are shaded in red.

Next we investigated PP_i- and ATP-dependent PFK activities in cellular fractions of *T. vaginalis*. Under anaerobic conditions, we detected specific PP_i-PFK activity of 0.4 to 0.9 μmol min^{-1} mg $protein^{-1}$ in the high-speed cytosolic fraction. Percoll-purified hydrogenosomes contained a low specific activity (~0.008 to 0.020 μmol min^{-1} mg $protein^{-1}$) of ATP-PFK. PP_i-PFK activity was not associated with the organelles. These results indicate that PP_i- and ATP-dependent PFK activities are present in *T. vaginalis* in two distinct cellular compartments, in the cytosol and in hydrogenosomes, respectively. However, the hydrogenosomal (ATP-dependent) activity is dwarfed by the well-characterized cytosolic PP_i-dependent activity, raising questions about the role of the ATP-dependent activity, if any, in core energy metabolism.

Expression of *Tv*ATP-PFK1 and ferredoxin 1 under the control of native promoters. The *T. vaginalis* SCSα promoter is a strong endogenous promoter for transient expression (42). The unexpected localization of *Tv*ATP-PFK1 when transiently expressed under the control of the SCSα promoter prompted us to test whether the promoter itself could influence the localization of the product. First, we tested SCSα versus the native promoter (NP) by determining the cellular localization of Fdx1, a model hydrogenosomal matrix protein that possesses a typical NTS (24), as well as an ITS (26). Full-length Fdx1 expressed under the control of the SCSα promoter localized to hydrogenosomes (Fig. 4). However, the expression of the same protein with a deleted NTS (ΔFdx1, with deletion of the first 8 amino acids, MLSQVCRF) resulted in a dual localization: the majority of the ΔFdx1 was accumulated in the cytosol, whereas a portion of the ΔFdx1 was targeted to the organelle. The matrix localization of ΔFdx1 was verified by a protease protection assay (Fig. 4). When the SCSα promoter was replaced with the native Fdx1 promoter (300 bp upstream of the coding sequence of the Fdx1 gene), the complete Fdx1 protein was imported into hydrogenosomes; however, Fdx1 with a deleted NTS remained in the cytosol (Fig. 4). It thus appears that the nature of the promoter that is used for protein expression may affect protein localization. In the case of Fdx1, the ITS is apparently not sufficient to deliver the protein into the organelles when the protein is expressed without NTS (ΔFdx1) under the control of the native promoter. Therefore, we also assessed the localization of the recombinant *Tv*ATP-PFK1 expressed in *T. vaginalis* under the control of its native *Tv*ATP-PFK1 promoter (Fig. 3). Immunofluorescence microscopy and Western blot analysis confirmed that under these conditions, *Tv*ATP-PFK1 was targeted into the hydrogenosomal matrix (Fig. 3).

***In vitro* import of *Tv*ATP-PFK1 into hydrogenosomes.** *Tv*ATP-PFK1 import into hydrogenosomes was investigated using an *in vitro* import system. *Tv*ATP-PFK1 labeled with ^{35}S was incubated with hydrogenosomes in import buffer supplemented with ATP and cytosolic extract for 0 to 60 min. After the incubation, the hydrogenosomes were treated with proteinase K to remove labeled proteins that were not imported into the organelles. These experiments revealed the time-dependent accumulation of radiolabeled *Tv*ATP-PFK1 within isolated hydrogenosomes (Fig. 5). Furthermore, we investigated whether ATP was necessary for import. When the import assay was supplemented with apyrase (20 U/ml), which converts ATP to AMP and pyrophosphate, no import of *Tv*ATP-PFK1 was observed (Fig. 5). This result indicates that NTS-independent import of *Tv*ATP-PFK1 requires ATP.

TvATP-PFK is recognized and imported into yeast mitochondria. It has been demonstrated that mitochondria and hydrogenosomes employ a common mode of NTS-dependent protein import (24). Thus, we were curious whether *Tv*ATP-PFK1 possesses an NTS-independent signal that is recognized by the protein import machinery of yeast mitochondria. We expressed *Tv*ATP-PFK1 with a C-terminal GFP tag in *S. cerevisiae*. Immunofluorescence microscopy showed that the GFP fusion protein colocalized with the mitochondrial marker MitoTracker (Fig. 6). A protease protection assay using isolated yeast mitochondria revealed that *Tv*ATP-PFK1 was imported into the organelle and excluded the possibility that the protein was associated with the mitochondrial surface. Cytochrome oxidase subunit VI was used as a control inner membrane protein. *Sc*ATP-PFK consists of an N-terminal extension of 200 aa, a catalytic domain of 359 aa, and a C-terminal regulatory domain (423 aa). When we expressed a full-length *Sc*ATP-PFK and a truncated form that lacked the C-terminal regulatory domain (1/2*Sc*PFK) in yeast, both recombinant proteins remained in the cytosol after translation (Fig. 6). The unique N-terminal extension of *Sc*PFK is rich in negatively charged amino acid residues (pI 4.67), which might prevent the targeting of the protein to mitochondria (43). Thus, we also ex-

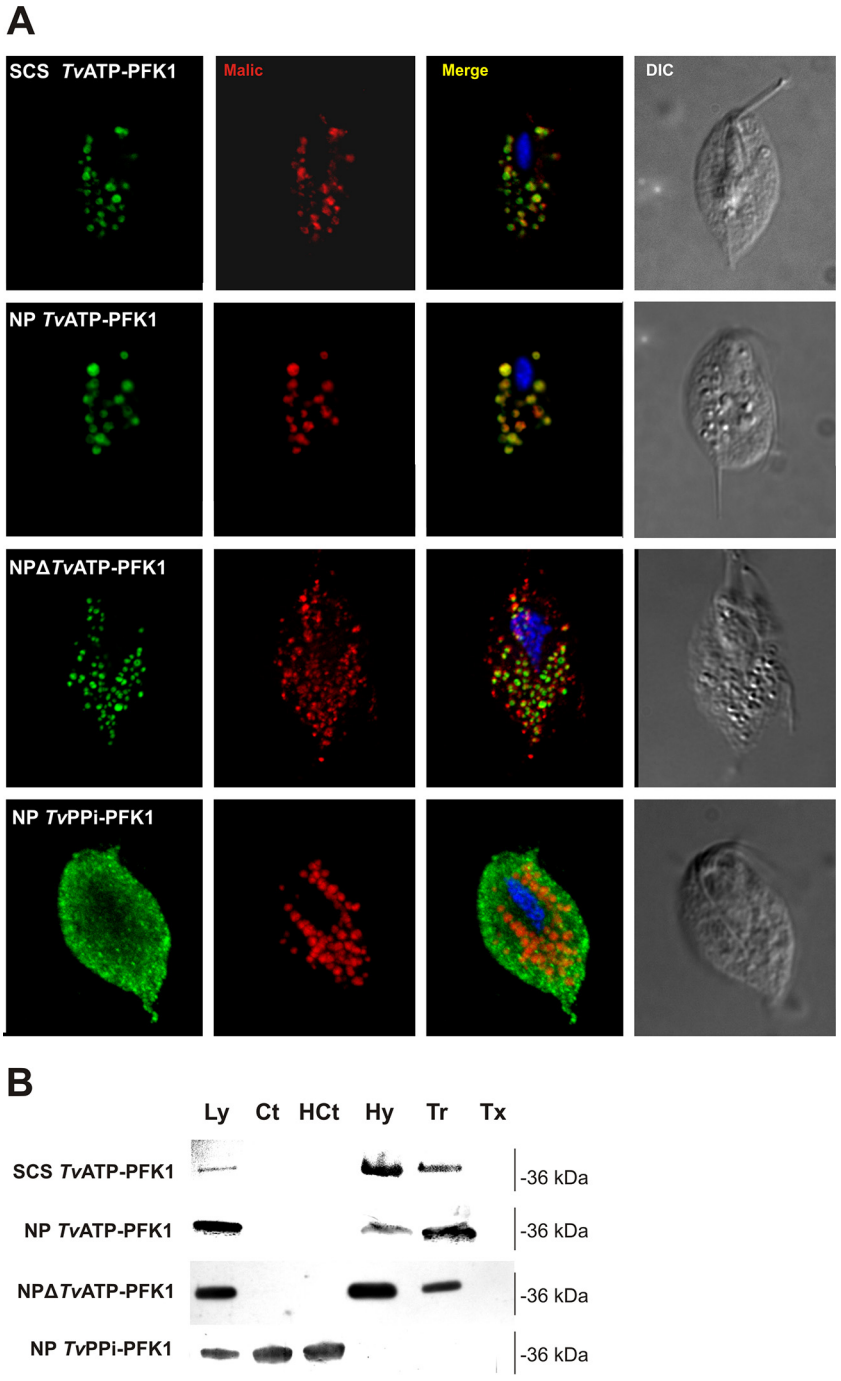

FIG 3 Cellular localization of ATP- and PP_i-dependent PFKs in *T. vaginalis*. (A) Immunofluorescence microscopy. Recombinant HA-tagged proteins were expressed in *T. vaginalis* cells and visualized using a monoclonal anti-HA antibody (green). *Tv*ATP-PFK1 and NP *Tv*ATP-PFK1 were expressed under the control of the strong SCSα promoter and the NP, respectively. NP Δ*Tv*ATP-PFK1 lacks 16 N-terminal amino acid residues. The hydrogenosomal marker protein malic enzyme was stained with a polyclonal rabbit antibody (red). The nucleus was stained using DAPI (4′,6-diamidino-2-phenylindole) (blue). DIC, differential interference contrast. (B) Protein protection assay. Hydrogenosomes were isolated from trichomonads expressing recombinant proteins with the C-terminal HA_2 tag and incubated with trypsin (Tr) or with trypsin and Triton X-100 (Tx). Samples were analyzed by immunoblotting using the monoclonal anti-HA tag antibody. Ly, total cell lysate; Ct, cytosol; HCt, high-speed cytosol; Hy, hydrogenosomes.

pressed the catalytic domain of *Sc*ATP-PFK, which is homologous to that of *Tv*ATP-PFK (ΔN1/2*Sc*PFK) alone. Interestingly, although some ΔN1/2*Sc*PFK signal was still observed in the cytosol, a significant portion was now also associated with the yeast mitochondrial membrane, as demonstrated by a protease protection assay (Fig. 6).

Collectively, these experiments show that *Tv*ATP-PFK1 possesses a targeting signal that is recognized by yeast mitochondria.

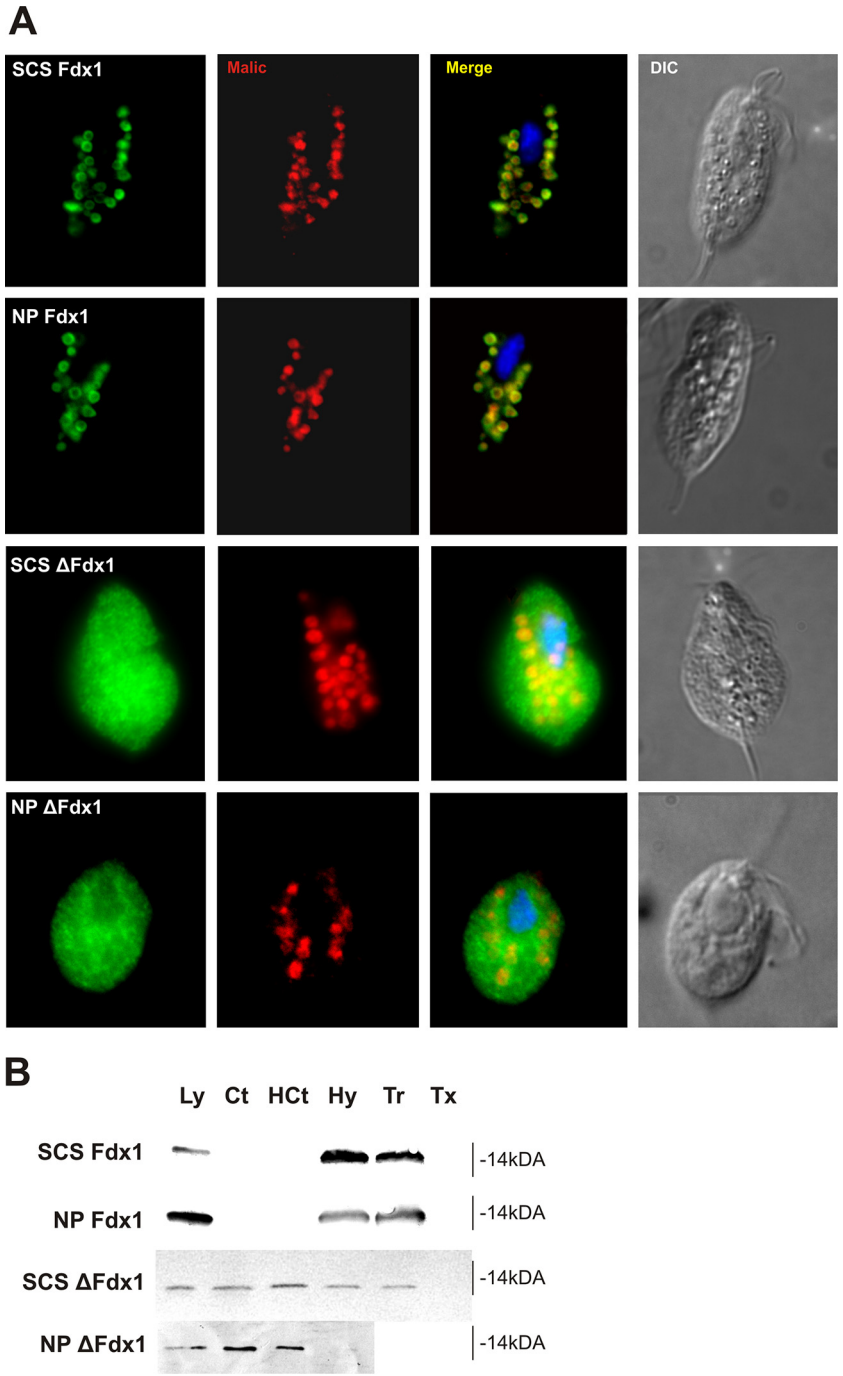

FIG 4 Effects of promoters on the cellular localization of ferredoxin. Fdx1 was used as a model protein with NTS-dependent targeting to test the effect of the SCSα promoter and the native promoter on Fdx1 localization. SCS Fdx1, Fdx1 (TVAG_003900) expressed under the control of the SCSα promoter; NP Fdx1, Fdx1 expressed under its native promoter; SCS ΔFdx1, Fdx1 with a deleted NTS that was expressed under the control of the SCSα promoter; NP ΔFdx1, ΔFdx1 expressed under the control of its native promoter. (A) Immunofluorescence microscopy. Recombinant HA-tagged proteins were expressed in *T. vaginalis* cells and visualized with monoclonal anti-HA antibody (green). The hydrogenosomal marker protein (malic enzyme) was detected using a polyclonal rabbit antibody (red). (B) Immunoblotting of subcellular fractions and protein protection assay. Ly, total cell lysate; Ct, cytosol; HCt, high-speed cytosol; Hy, hydrogenosomes; Tr, hydrogenosomes treated with trypsin; Tx, hydrogenosomal fraction treated with trypsin and Triton X-100.

The complete *Sc*ATP-PFK is retained in the cytosol, but the catalytic portion of *Sc*ATP-PFK displays mitochondrial membrane affinity.

Cellular localization of heterologous ATP-PFKs in *T. vaginalis*. We tested whether the hydrogenosomal protein import machinery can import heterologous ATP-PFKs. When we expressed complete *Sc*ATP-PFK in *T. vaginalis* under the control of the *Tv*ATP-PFK1 promoter, immunofluorescence microscopy revealed predominantly cytosolic localization of the protein, although the protein partially localized to hydrogenosomes (Fig. 7).

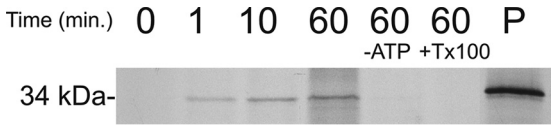

FIG 5 *In vitro* import of *Tv*ATP-PFK1 into hydrogenosomes. *In vitro*-synthesized ^{35}S-radiolabeled *Tv*ATP-PFK1 protein was incubated with isolated hydrogenosomes in import buffer at 25°C for 1, 10, and 60 min. At each time point, surface-associated proteins were degraded with proteinase K. Radiolabeled precursor was not imported in the absence of ATP (−ATP), depleted by addition of apyrase. A control for proteinase K activity was performed by the addition of Triton X-100 to the sample after 60 min of protein import (+Tx100). P, radiolabeled *Tv*ATP-PFK1 precursor protein. The samples were analyzed by SDS-PAGE and autoradiography.

The expression of 1/2*Sc*PFK revealed that the N-terminal half of *Sc*ATP-PFK was mainly associated with hydrogenosomes; however, the hydrogenosomal labeling was rather irregular in comparison to the labeling of malic enzyme, which was used as a control matrix protein. Western blot analysis of cellular fractions confirmed that both *Sc*ATP-PFK and 1/2*Sc*PFK were present in the cytosolic fractions (low- and high-speed cytosolic fractions). Parts of both proteins were also associated with the hydrogenosomal fractions; however, the signals disappeared after trypsin treatment. When we expressed only the catalytic part of the yeast enzyme lacking the negatively charged N-terminal sequence (ΔN1/2*Sc*PFK), a significant portion of the protein appeared inside the hydrogenosomes (Fig. 7). Next, we were interested in whether the targeting information is also present in short *E. coli* ATP-PFK orthologues that display 42% amino acid sequence identity with *Tv*ATP-PFKs. Thus, we expressed *Ec*ATP-PFK under the control of the *Tv*ATP-PFK1 promoter. Under these conditions, the *E. coli* protein was detected in the cytosol, and in part, it was associated with the hydrogenosomal surface (Fig. 7). However, when expressed under the SCSα promoter, a significant part of the protein was imported into the hydrogenosomes.

DISCUSSION

We investigated the cellular localization and NTS-independent import of *Tv*ATP-PFK into *T. vaginalis* hydrogenosomes. The parasite expresses both PP_i- and ATP-dependent enzymes, which are compartmentalized in the cytosol and hydrogenosomes, respectively. The classical PP_i-dependent activity of the parasite is about 50-fold higher than the newly characterized ATP-dependent activity, rendering the metabolic significance of the latter unclear. A phylogenetic analysis revealed that both types of PFKs are present across the parabasalids sampled so far. *Tv*ATP-PFK corresponds to a "short" ~35-kDa form of bacterial PFK that consists of only a catalytic domain, whereas the C-terminal regulatory domain typical of opisthokont ATP-PFKs is lacking. The targeting of *Tv*ATP-PFK1 to hydrogenosomes appears to be a

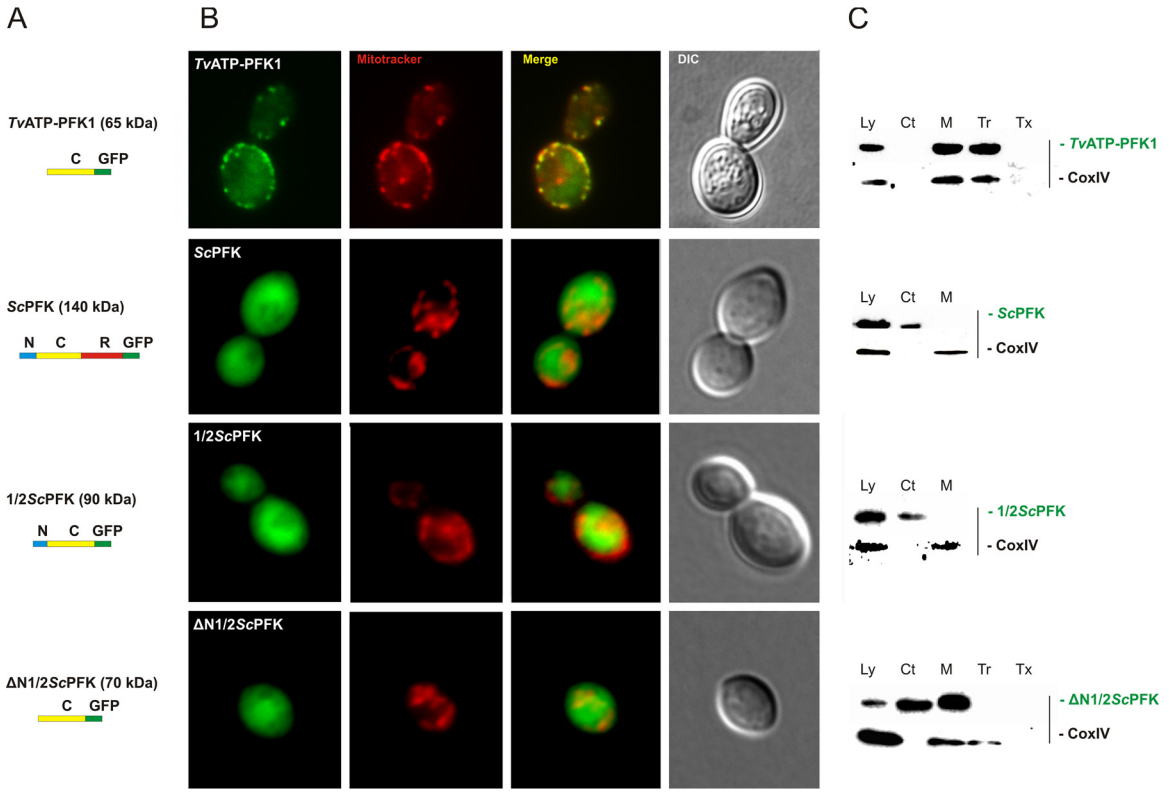

FIG 6 Cellular localization of *Tv*ATP-PFK1 and yeast ATP-PFK in *S. cerevisiae*. (A) Domain structure of the expressed proteins. N, N-terminal extension; C, catalytic domain; R, regulatory domain; GFP, green fluorescent protein tag. (B) Immunofluorescence microscopy. *Tv*ATP-PFK1 was expressed in yeasts with C-terminal GFP (green). Mitochondria were detected using MitoTracker dye (Invitrogen) (red). *Tv*ATP-PFK1, complete short *T. vaginalis* PFK; *Sc*PFK, complete long yeast PFK; 1/2*Sc*PFK, N-terminal extension (205 aa) and catalytic domain (359 aa) of *Sc*PFK; ΔN1/2*Sc*PFK, catalytic domain with deleted N-terminal extension. (C) Immunoblotting of subcellular fractions and protein protection assay. GFP-tagged proteins were detected using an anti-GFP antibody. Cytochrome oxidase subunit IV (CoxIV) was used as a mitochondrial marker, which was detected using a rabbit anti-CoxIV antibody. Ly, total cell lysate; Ct, cytosol; M, mitochondria; Tr, hydrogenosomes treated with trypsin; Tx, hydrogenosomal fraction treated with trypsin and Triton X-100.

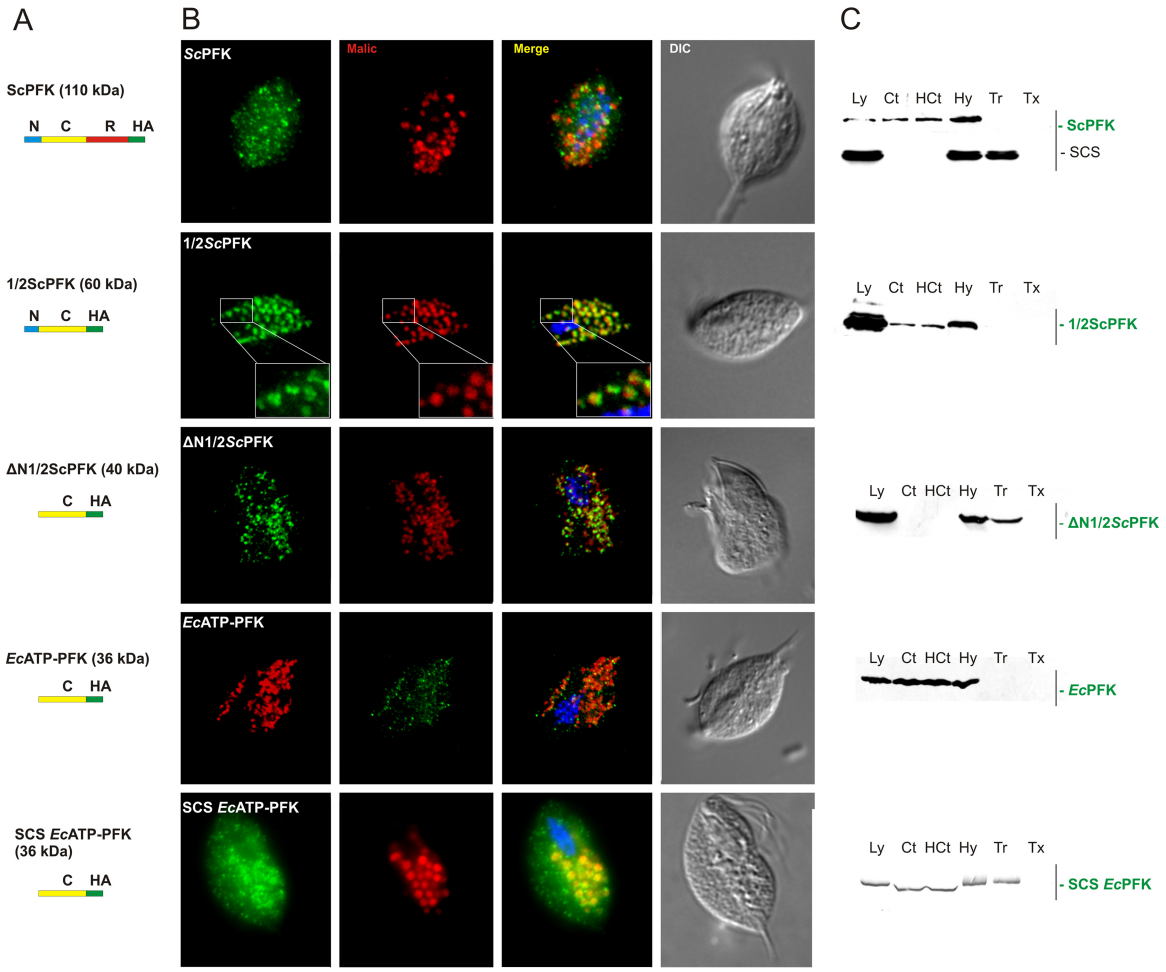

FIG 7 Cellular localization of *S. cerevisiae Sc*ATP-PFK and *Ec*ATP-PFK in *T. vaginalis*. (A) Domain structure of the expressed constructs. N, N-terminal extension; C, catalytic domain; R, regulatory domain; HA, hemagglutinin tag. (B) Recombinant HA-tagged proteins were expressed in *T. vaginalis* cells under the control of the *Tv*ATP-PFK1 promoter. SCS *Ec*ATP-PFK was expressed under the control of the SCSα promoter. HA-tagged proteins were visualized with mouse monoclonal anti-HA antibody (green). The hydrogenosomal marker protein (malic enzyme) was detected using a polyclonal rabbit antibody (red). (C) Immunoblotting of subcellular fractions and protein protection assay. Recombinant HA-tagged proteins were detected using monoclonal anti-HA antibody. The hydrogenosomal marker protein SCSα was detected using a rabbit polyclonal antibody. Ly, total cell lysate; Ct, cytosol; HCt, high-speed cytosol; Hy, hydrogenosomes; Tr, hydrogenosomes treated with trypsin; Tx, hydrogenosomal fraction treated with trypsin and Triton X-100.

highly specific and ATP-dependent process, even though the protein is not predicted to possess a cleavable NTS, which is typical of hydrogenosomal matrix proteins (44, 45).

The replacement of ATP with PP_i as a phosphate donor in the phosphorylation of fructose-6-phosphate allows an increased glycolytic ATP yield (3), conceivably a significant feature for a fermenting organism. Examples of organisms that express both PP_i-PFK and ATP-PFK are rare. The actinomycete *Amycolatopsis methanolica* possesses both genes, but their expression depends strictly on the carbon source (46). *Entamoeba histolytica* possesses two genes for PP_i-PFK orthologues; however, one of the gene products has been shown to utilize ATP instead of PP_i, and it has been suggested that the two enzymes might be expressed during different life stages (37). In plants, PP_i-PFK and ATP-PFK are both cytosolic enzymes with reciprocal expression responding to environmental perturbations (47). Whereas the expression of PP_i-PFK is upregulated by anoxia or orthophosphate deficiency, ATP-PFK is downregulated under such conditions. The spatial separation in *T. vaginalis* of PP_i-PFK and ATP-PFK to the cytosol and hydrogenosomes, respectively, could be an alternative solution to avoid interference between the two enzymes.

Specific targeting of *Tv*ATP-PFK to the organelle was demonstrated *in vivo* by episomal expression of tagged *Tv*ATP-PFK1 under SCSα and its native promoters, as well as the *in vitro* import of radiolabeled protein into isolated hydrogenosomes. Through the HA-tagged *Tv*ATP-PFK1, products of four paralogous *Tv*ATP-PFK genes were immunoprecipitated from isolated hydrogenosomes and identified by mass spectrometry. Earlier proteomic studies suggested association of the glycolytic pathway, including *Tv*ATP-PFK, with the hydrogenosome (13, 15), which raises the question of whether glycolytic enzymes form functional protein complexes on the hydrogenosomal outer membrane, as has been shown for mitochondria. For example, in *Arabidopsis thaliana*, 5 to 10% of each glycolytic enzyme is associated with the outer mitochondrial surface. Mammalian and fish heart mitochondria bind hexokinase and ATP-PFK (48), which has been discussed in the context of an increased glycolytic rate under hypoxic conditions (49). However, in *T. vaginalis*, expression of seven glycolytic

enzymes, including PP_i-PFK, showed exclusively cytosolic localization of these proteins (15, 26). Moreover, available cell fractionation studies of glyceraldehyde-3-phosphate dehydrogenase (50) and PP_i-PFK (this study) indicated that the corresponding activities are not associated with the organelle. These data do not support the formation of functional glycolytic complexes at the hydrogenosomal membrane and make the interpretation of previous proteomic analysis problematic, although systematic studies of glycolytic enzyme activities in cellular fractions of *T. vaginalis* are currently lacking. The localization of *Tv*ATP-PFK in the hydrogenosomal matrix, as shown in this study, is new for trichomonads.

Organellar forms of ATP-PFK have been found in glycosomes (51) and chloroplasts (52) thus far, where ATP-PFK operates within a known biochemical context. Kinetoplastids catalyze the "upper" six glycolytic steps in glycosomes, exporting 3-phosphoglycerate to the cytosol. Microalgae, such as *Chlamydomonas reinhardtii*, possess four glycolytic enzymes that convert glucose to glyceraldehyde-3-phosphate in chloroplasts, whereas the rest of glycolysis is localized in the cytosol (7). The most complicated glycolytic network has been found in diatoms, such as *P. tricornutum*, in which the complete set of glycolytic enzymes is present in the cytosol; nine glycolytic enzymes, including ATP-PFK, catalyze the conversion of glucose-1-phosphate to pyruvate in the chloroplast, and five glycolytic enzymes convert glyceraldehyde-3-phospate to pyruvate in the mitochondrion (8). In these organisms, the specific targeting of various glycolytic enzymes into the organelles is mediated by NTS (mitochondria), peroxisomal targeting signals (glycosomes), and plastid targeting signal (chloroplasts). The organellar *Tv*ATP-PFK found in *T. vaginalis* is unique with respect to three features: (i) it is a single glycolytic enzyme that is compartmentalized without apparent distal and proximal partners in the pathway, (ii) it is the only PFK that was observed to be imported into mitochondrion-related organelles, and (iii) the import into hydrogenosomes is mediated by ITS. The overall low hydrogenosomal ATP-PFK activity (approximately 2% of the PP_i-dependent activity), together with the lack of organellar glycolytic partners, raises questions regarding the metabolic role of *Tv*ATP-PFK and whether another function, unrelated to glycolysis, might be a possible alternative. Various moonlighting functions have been suggested for ATP-PFK in eukaryotes and bacteria, such as participation in the microautophagy of peroxisomes (53), RNA processing and degradation (54), and surface binding of plasminogen (55) and mannan (56). In our view, however, none of these functions currently appear likely for *Tv*ATP-PFK.

Heterologous expression of *Tv*ATP-PFK1 in *S. cerevisiae* revealed that the trichomonad enzyme is imported into yeast mitochondria, in addition to hydrogenosomes. This result indicates that *Tv*ATP-PFK1 possesses a targeting signal that is recognized by the hydrogenosomal, as well as the mitochondrial, import machinery. From an evolutionary perspective, these data suggest that the "short" ancient ATP-PFK might be predisposed to being recognized and imported into mitochondria, which might be a relict from the early phases of mitochondrial evolution. If so, the evolving eukaryotic cell had not only to develop a mechanism for retargeting nuclear-encoded proteins to mitochondria, but also to prevent the organellar translocation of some proteins, such as ATP-PFK, that are components of cytosolic pathways. Interestingly, unlike short bacterial ATP-PFK, eukaryotes frequently possess structurally modified long ATP-PFK that consists of catalytic and regulatory domains. In addition, the ATP-PFK of yeast and other fungi is equipped with a negatively charged N-terminal extension that may interfere with organellar import. Indeed, when we expressed the catalytic domain of *Sc*ATP-PFK with the N-terminal extension (1/2*Sc*PFK) in *T. vaginalis*, the protein was not delivered to the hydrogenosomal matrix, indicating that the extension prevents translocation. However, the hydrogenosomal import machinery was able to recognize and partially import truncated yeast *Sc*ATP-PFK, consisting of only the catalytic domain (ΔN1/2ScPFK), and the short proteobacterial *Ec*ATP-PFK, which are both homologous to *Tv*ATP-PFK. These results are consistent with the idea that ancient ATP-PFKs were predisposed to target the organelle. They also support previous analysis of proteins encoded by *E. coli* that predicted the presence of mitochondrial targeting information in about 5% of bacterial proteins (57).

The cell localization studies performed need to be interpreted with caution. Import of *Ec*ATP-PFK was observed when the gene was expressed under a strong SCSα promoter, while expression under the *Tv*ATP-PFK1 promoter resulted in partial association of *Tv*ATP-PFK1 with the outer hydrogenosomal membrane. Similarly, we observed promoter-dependent variation in the cell localization of Fdx, which possesses both NTS and ITS. Although we cannot exclude the possibility that hydrogenosomal localization of proteins expressed under strong promoters reflects protein mislocalization, it has been shown previously that six glycolytic enzymes expressed under the SCSα promoter remained exclusively in the cytosol, as expected, which argues against protein mislocalization (26). Therefore, it is more likely that, in addition to ITS, a suitable level of protein is required for protein translocation into the hydrogenosomes, while proteins without ITS are not targeted to the organelle regardless of the protein level. Importantly, expression of ΔN1/2ScPFK under *Tv*ATP-PFK1 was sufficient for its partial translocation into hydrogenosomes.

In conclusion, we identified ATP-PFK in *T. vaginalis* that is efficiently delivered into mitochondria and hydrogenosomes via NTS-independent mechanisms. Although NTS-independent targeting of membrane proteins is well documented, little is known about NTS-independent targeting of soluble proteins and the characters of multiple inner signals that are embedded within the protein structure (23, 58). The import of ATP-PFK into *T. vaginalis* hydrogenosomes can be used to investigate the molecular mechanisms that facilitate NTS-independent targeting and underpins the importance of internal targeting motifs that, in the case of PFK, are recognized in species spanning different eukaryotic supergroups. Intriguingly, the function of *Tv*ATP-PFK in *T. vaginalis* hydrogenosomes remains mysterious.

ACKNOWLEDGMENTS

This work was supported by the Czech Grant Foundation (13-09208J); the Biomedicine Centre of the Academy of Sciences and Charles University, Prague, Czech Republic (CZ.1.05/1.1.00/02.0109), from the European Regional Development Fund, project no. CZ.1.07/2.3.00/30.0061 (OPVK); and DFG grants to S.B.G. (GO1825/3–1). S.B.G. was additionally supported by a DFG grant to William F. Martin (MA1426/19-1).

REFERENCES

1. **Lane N, Martin W.** 2010. The energetics of genome complexity. Nature **467:**929–934. http://dx.doi.org/10.1038/nature09486.
2. **Hannaert V, Brinkmann H, Nowitzki U, Lee JA, Albert MA, Sensen CW, Gaasterland T, Muller M, Michels P, Martin W.** 2000. Enolase from *Trypanosoma brucei*, from the amitochondriate protist *Mastiga-*

moeba balamuthi, and from the chloroplast and cytosol of *Euglena gracilis*: pieces in the evolutionary puzzle of the eukaryotic glycolytic pathway. Mol Biol Evol **17:**989–1000. http://dx.doi.org/10.1093/oxfordjournals.molbev.a026395.

3. **Müller M, Mentel M, van Hellemond JJ, Henze K, Woehle C, Gould SB, Yu RY, van der Giezen M, Tielens AG, Martin WF.** 2012. Biochemistry and evolution of anaerobic energy metabolism in eukaryotes. Microbiol Mol Biol Rev **76:**444–495. http://dx.doi.org/10.1128/MMBR.05024-11.
4. **Embley TM, Martin W.** 2006. Eukaryotic evolution, changes and challenges. Nature **440:**623–630. http://dx.doi.org/10.1038/nature04546.
5. **Gualdron-Lopez M, Brennand A, Hannaert V, Quinones W, Caceres AJ, Bringaud F, Concepcion JL, Michels PA.** 2012. When, how and why glycolysis became compartmentalised in the Kinetoplastea. A new look at an ancient organelle. Int J Parasitol **42:**1–20. http://dx.doi.org/10.1016/j.ijpara.2011.10.007.
6. **Schnarrenberger C, Pelzer-Reith B, Yatsuki H, Freund S, Jacobshagen S, Hori K.** 1994. Expression and sequence of the only detectable aldolase in *Chlamydomonas reinhardtii*. Arch Biochem Biophys **313:**173–178. http://dx.doi.org/10.1006/abbi.1994.1374.
7. **Johnson X, Alric J.** 2013. Central carbon metabolism and electron transport in *Chlamydomonas reinhardtii*: metabolic constraints for carbon partitioning between oil and starch. Eukaryot Cell **12:**776–793. http://dx.doi.org/10.1128/EC.00318-12.
8. **Kroth PG, Chiovitti A, Gruber A, Martin-Jezequel V, Mock T, Parker MS, Stanley MS, Kaplan A, Caron L, Weber T, Maheswari U, Armbrust EV, Bowler C.** 2008. A model for carbohydrate metabolism in the diatom *Phaeodactylum tricornutum* deduced from comparative whole genome analysis. PLoS One **3:**e1426. http://dx.doi.org/10.1371/journal.pone.0001426.
9. **Nakayama T, Ishida K, Archibald JM.** 2012. Broad distribution of TPI-GAPDH fusion proteins among eukaryotes: evidence for glycolytic reactions in the mitochondrion? PLoS One **7:**e52340. http://dx.doi.org/10.1371/journal.pone.0052340.
10. **Mertens E, Ladror US, Lee JA, Miretsky A, Morris A, Rozario C, Kemp RG, Müller M.** 1998. The pyrophosphate-dependent phosphofructokinase of the protist, Trichomonas vaginalis, and the evolutionary relationships of protist phosphofructokinases. J Mol Evol **47:**739–750. http://dx.doi.org/10.1007/PL00006433.
11. **Winkler C, Delvos B, Martin W, Henze K.** 2007. Purification, microsequencing and cloning of spinach ATP-dependent phosphofructokinase link sequence and function for the plant enzyme. FEBS J **274:**429–438. http://dx.doi.org/10.1111/j.1742-4658.2006.05590.x.
12. **Carlton JM, Hirt RP, Silva JC, Delcher AL, Schatz M, Zhao Q, Wortman JR, Bidwell SL, Alsmark UC, Besteiro S, Sicheritz-Ponten T, Noel CJ, Dacks JB, Foster PG, Simillion C, Van de PY, Miranda-Saavedra D, Barton GJ, Westrop GD, Muller S, Dessi D, Fiori PL, Ren Q, Paulsen I, Zhang H, Bastida-Corcuera FD, Simoes-Barbosa A, Brown MT, Hayes RD, Mukherjee M, Okumura CY, Schneider R, Smith AJ, Vanacova S, Villalvazo M, Haas BJ, Pertea M, Feldblyum TV, Utterback TR, Shu CL, Osoegawa K, de Jong PJ, Hrdy I, Horvathova L, Zubacova Z, Dolezal P, Malik SB, Logsdon JM, Jr, Henze K, Gupta A, Wang CC, Dunne RL, Upcroft JA, Upcroft P, White O, Salzberg SL, Tang P, Chiu CH, Lee YS, Embley TM, Coombs GH, Mottram JC, Tachezy J, Fraser-Liggett CM, Johnson PJ.** 2007. Draft genome sequence of the sexually transmitted pathogen *Trichomonas vaginalis*. Science **315:**207–212. http://dx.doi.org/10.1126/science.1132894.
13. **Schneider RE, Brown MT, Shiflett AM, Dyall SD, Hayes RD, Xie Y, Loo JA, Johnson PJ.** 2011. The *Trichomonas vaginalis* hydrogenosome proteome is highly reduced relative to mitochondria, yet complex compared with mitosomes. Int J Parasitol **41:**1421–1434. http://dx.doi.org/10.1016/j.ijpara.2011.10.001.
14. **Henze K.** 2007. The proteome of *T. vaginalis* hydrogenosomes, p 163–178. *In* Tachezy J (ed), Hydrogenosomes and mitosomes: mitochondria of anaerobic eukaryotes. Springer, Berlin, Germany.
15. **Rada P, Dolezal P, Jedelsky PL, Bursac D, Perry AJ, Sedinova M, Smiskova K, Novotny M, Beltran NC, Hrdy I, Lithgow T, Tachezy J.** 2011. The core components of organelle biogenesis and membrane transport in the hydrogenosomes of *Trichomonas vaginalis*. PLoS One **6:**e24428. http://dx.doi.org/10.1371/journal.pone.0024428.
16. **Liapounova NA, Hampl V, Gordon PM, Sensen CW, Gedamu L, Dacks JB.** 2006. Reconstructing the mosaic glycolytic pathway of the anaerobic eukaryote Monocercomonoides. Eukaryot Cell **5:**2138–2146. http://dx.doi.org/10.1128/EC.00258-06.
17. **Bapteste E, Moreira D, Philippe H.** 2003. Rampant horizontal gene transfer and phospho-donor change in the evolution of the phosphofructokinase. Gene **318:**185–191. http://dx.doi.org/10.1016/S0378-1119(03)00797-2.
18. **Shirakihara Y, Evans PR.** 1988. Crystal structure of the complex of phosphofructokinase from *Escherichia coli* with its reaction products. J Mol Biol **204:**973–994. http://dx.doi.org/10.1016/0022-2836(88)90056-3.
19. **Poorman RA, Randolph A, Kemp RG, Heinrikson RL.** 1984. Evolution of phosphofructokinase: gene duplication and creation of new effector sites. Nature **309:**467–469. http://dx.doi.org/10.1038/309467a0.
20. **Mony BM, Mehta M, Jarori GK, Sharma S.** 2009. Plant-like phosphofructokinase from *Plasmodium falciparum* belongs to a novel class of ATP-dependent enzymes. Int J Parasitol **39:**1441–1453. http://dx.doi.org/10.1016/j.ijpara.2009.05.011.
21. **Vogtle FN, Wortelkamp S, Zahedi RP, Becker D, Leidhold C, Gevaert K, Kellermann J, Voos W, Sickmann A, Pfanner N, Meisinger C.** 2009. Global analysis of the mitochondrial N-proteome identifies a processing peptidase critical for protein stability. Cell **139:**428–439. http://dx.doi.org/10.1016/j.cell.2009.07.045.
22. **Gakh O, Cavadini P, Isaya G.** 2002. Mitochondrial processing peptidases. Biochim Biophys Acta **1592:**63–77. http://dx.doi.org/10.1016/S0167-4889(02)00265-3.
23. **Chacinska A, Koehler CM, Milenkovic D, Lithgow T, Pfanner N.** 2009. Importing mitochondrial proteins: machineries and mechanisms. Cell **138:**628–644. http://dx.doi.org/10.1016/j.cell.2009.08.005.
24. **Bradley PJ, Lahti CJ, Plumper E, Johnson PJ.** 1997. Targeting and translocation of proteins into the hydrogenosome of the protist Trichomonas: similarities with mitochondrial protein import. EMBO J **16:**3484–3493. http://dx.doi.org/10.1093/emboj/16.12.3484.
25. **Dolezal P, Smid O, Rada P, Zubacova Z, Bursac D, Sutak R, Nebesarova J, Lithgow T, Tachezy J.** 2005. Giardia mitosomes and trichomonad hydrogenosomes share a common mode of protein targeting. Proc Natl Acad Sci U S A **102:**10924–10929. http://dx.doi.org/10.1073/pnas.0500349102.
26. **Zimorski V, Major P, Hoffmann K, Bras XP, Martin WF, Gould SB.** 2013. The N-terminal sequences of four major hydrogenosomal proteins are not essential for import into hydrogenosomes of *Trichomonas vaginalis*. J Eukaryot Microbiol **60:**89–97. http://dx.doi.org/10.1111/jeu.12012.
27. **Mentel M, Zimorski V, Haferkamp P, Martin W, Henze K.** 2008. Protein import into hydrogenosomes of *Trichomonas vaginalis* involves both N-terminal and internal targeting signals: a case study of thioredoxin reductases. Eukaryot Cell **7:**1750–1757. http://dx.doi.org/10.1128/EC.00206-08.
28. **Katoh K, Kuma K, Toh H, Miyata T.** 2005. MAFFT version 5: improvement in accuracy of multiple sequence alignment. Nucleic Acids Res **33:**511–518. http://dx.doi.org/10.1093/nar/gki198.
29. **Hall TA.** 1999. BioEdit: a user-friendly biological sequence alignment editor and analysis program for Windows 95/98/NT. Nucleic Acids Symp Ser **41:**95–98.
30. **Stamatakis A.** 2006. RAxML-VI-HPC: maximum likelihood-based phylogenetic analyses with thousands of taxa and mixed models. Bioinformatics **22:**2688–2690. http://dx.doi.org/10.1093/bioinformatics/btl446.
31. **Stamatakis A, Hoover P, Rougemont J.** 2008. A rapid bootstrap algorithm for the RAxML Web servers. Syst Biol **57:**758–771. http://dx.doi.org/10.1080/10635150802429642.
32. **Lartillot N, Rodrigue N, Stubbs D, Richer J.** 2013. PhyloBayes MPI: phylogenetic reconstruction with infinite mixtures of profiles in a parallel environment. Syst Biol **62:**611–615. http://dx.doi.org/10.1093/sysbio/syt022.
33. **Hrdy I, Hirt RP, Dolezal P, Bardonova L, Foster PG, Tachezy J, Embley TM.** 2004. Trichomonas hydrogenosomes contain the NADH dehydrogenase module of mitochondrial complex I. Nature **432:**618–622. http://dx.doi.org/10.1038/nature03149.
34. **Niedenthal RK, Riles L, Johnston M, Hegemann JH.** 1996. Green fluorescent protein as a marker for gene expression and subcellular localization in budding yeast. Yeast **12:**773–786.
35. **Sutak R, Dolezal P, Fiumera HL, Hrdy I, Dancis A, Delgadillo-Correa MG, Johnson PJ, Müller M, Tachezy J.** 2004. Mitochondrial-type assembly of FeS centers in the hydrogenosomes of the amitochondriate eukaryote *Trichomonas vaginalis*. Proc Natl Acad Sci U S A **101:**10368–10373. http://dx.doi.org/10.1073/pnas.0401319101.
36. **Drmota T, Proost P, Van Ranst M, Weyda F, Kulda J, Tachezy J.** 1996. Iron-ascorbate cleavable malic enzyme from hydrogenosomes of

Trichomonas vaginalis: purification and characterization. Mol Biochem Parasitol **83:**221–234. http://dx.doi.org/10.1016/S0166-6851(96)02777-6.

37. **Chi AS, Deng Z, Albach RA, Kemp RG.** 2001. The two phosphofructokinase gene products of *Entamoeba histolytica*. J Biol Chem **276:**19974–19981. http://dx.doi.org/10.1074/jbc.M011584200.
38. **Mertens E, Van Schaftingen E, Müller M.** 1989. Presence of a fructose-2,6-bisphosphate-insensitive pyrophosphate: fructose-6-phosphate phosphotransferase in the anaerobic protozoa *Tritrichomonas foetus*, *Trichomonas vaginalis* and *Isotricha prostoma*. Mol Biochem Parasitol **37:**183–190. http://dx.doi.org/10.1016/0166-6851(89)90150-3.
39. **Gregg C, Kyryakov P, Titorenko VI.** 2009. Purification of mitochondria from yeast cells. J Vis Exp **30:**1417. http://dx.doi.org/10.3791/1417.
40. **Michels PA, Chevalier N, Opperdoes FR, Rider MH, Rigden DJ.** 1997. The glycosomal ATP-dependent phosphofructokinase of *Trypanosoma brucei* must have evolved from an ancestral pyrophosphate-dependent enzyme. Eur J Biochem **250:**698–704. http://dx.doi.org/10.1111/j.1432-1033.1997.00698.x.
41. **Mustroph A, Sonnewald U, Biemelt S.** 2007. Characterisation of the ATP-dependent phosphofructokinase gene family from *Arabidopsis thaliana*. FEBS Lett **581:**2401–2410. http://dx.doi.org/10.1016/j.febslet.2007.04.060.
42. **Delgadillo MG, Liston DR, Niazi K, Johnson PJ.** 1997. Transient and selectable transformation of the parasitic protist *Trichomonas vaginalis*. Proc Natl Acad Sci U S A **94:**4716–4720. http://dx.doi.org/10.1073/pnas.94.9.4716.
43. **Gerber J, Neumann K, Prohl C, Muhlenhoff U, Lill R.** 2004. The yeast scaffold proteins Isu1p and Isu2p are required inside mitochondria for maturation of cytosolic Fe/S proteins. Mol Cell Biol **24:**4848–4857. http://dx.doi.org/10.1128/MCB.24.11.4848-4857.2004.
44. **Smid O, Matuskova A, Harris SR, Kucera T, Novotny M, Horvathova L, Hrdy I, Kutejova E, Hirt RP, Embley TM, Janata J, Tachezy J.** 2008. Reductive evolution of the mitochondrial processing peptidases of the unicellular parasites *Trichomonas vaginalis* and *Giardia intestinalis*. PLoS Pathog **4:**e1000243. http://dx.doi.org/10.1371/journal.ppat.1000243.
45. **Burstein D, Gould SB, Zimorski V, Kloesges T, Kiosse F, Major P, Martin WF, Pupko T, Dagan T.** 2012. A machine learning approach to identify hydrogenosomal proteins in *Trichomonas vaginalis*. Eukaryot Cell **11:**217–228. http://dx.doi.org/10.1128/EC.05225-11.
46. **Alves AM, Euverink GJ, Santos H, Dijkhuizen L.** 2001. Different physiological roles of ATP- and PP(i)-dependent phosphofructokinase isoenzymes in the methylotrophic actinomycete *Amycolatopsis methanolica*. J Bacteriol **183:**7231–7240. http://dx.doi.org/10.1128/JB.183.24.7231-7240.2001.
47. **Plaxton WC, Tran HT.** 2011. Metabolic adaptations of phosphate-starved plants. Plant Physiol **156:**1006–1015. http://dx.doi.org/10.1104/pp.111.175281.
48. **Treberg JR, MacCormack TJ, Lewis JM, Almeida-Val VM, Val AL, Driedzic WR.** 2007. Intracellular glucose and binding of hexokinase and phosphofructokinase to particulate fractions increase under hypoxia in heart of the Amazonian armored catfish (*Liposarcus pardalis*). Physiol Biochem Zool **80:**542–550. http://dx.doi.org/10.1086/520129.
49. **Graham JW, Williams TC, Morgan M, Fernie AR, Ratcliffe RG, Sweetlove LJ.** 2007. Glycolytic enzymes associate dynamically with mitochondria in response to respiratory demand and support substrate channeling. Plant Cell **19:**3723–3738. http://dx.doi.org/10.1105/tpc.107.053371.
50. **Markos A, Miretsky A, Müller M.** 1993. A glyceraldehyde-3-phosphate dehydrogenase with eubacterial features in the amitochondriate eukaryote, *Trichomonas vaginalis*. J Mol Evol **37:**631–643. http://dx.doi.org/10.1007/BF00182749.
51. **Opperdoes FR, Borst P.** 1977. Localization of nine glycolytic enzymes in a microbody-like organelle in *Trypanosoma brucei*: the glycosome. FEBS Lett **80:**360–364. http://dx.doi.org/10.1016/0014-5793(77)80476-6.
52. **Plaxton WC.** 1996. The organization and regulation of plant glycolysis. Annu Rev Plant Physiol Plant Mol Biol **47:**185–214. http://dx.doi.org/10.1146/annurev.arplant.47.1.185.
53. **Gancedo C, Flores CL, Gancedo JM.** 2014. Evolution of moonlighting proteins: insight from yeasts. Biochem Soc Trans **42:**1715–1719. http://dx.doi.org/10.1042/BST20140199.
54. **Commichau FM, Rothe FM, Herzberg C, Wagner E, Hellwig D, Lehnik-Habrink M, Hammer E, Volker U, Stulke J.** 2009. Novel activities of glycolytic enzymes in *Bacillus subtilis*: interactions with essential proteins involved in mRNA processing. Mol Cell Proteomics **8:**1350–1360. http://dx.doi.org/10.1074/mcp.M800546-MCP200.
55. **Kinnby B, Booth NA, Svensater G.** 2008. Plasminogen binding by oral streptococci from dental plaque and inflammatory lesions. Microbiology **154:**924–931. http://dx.doi.org/10.1099/mic.0.2007/013235-0.
56. **Katakura Y, Sano R, Hashimoto T, Ninomiya K, Shioya S.** 2010. Lactic acid bacteria display on the cell surface cytosolic proteins that recognize yeast mannan. Appl Microbiol Biotechnol **86:**319–326. http://dx.doi.org/10.1007/s00253-009-2295-y.
57. **Lucattini R, Likic VA, Lithgow T.** 2004. Bacterial proteins predisposed for targeting to mitochondria. Mol Biol Evol **21:**652–658. http://dx.doi.org/10.1093/molbev/msh058.
58. **Garg S, Stolting J, Zimorski V, Rada P, Tachezy J, Martin WF, Gould SB.** 2015. Conservation of transit peptide-independent protein import into the mitochondrial and hydrogenosomal matrix. Genome Biol Evol **7:**2716–2726. http://dx.doi.org/10.1093/gbe/evv175.